Cancer Management and Research

Dovepress

open access to scientific and medical research

Open Access Full Text Article

ORIGINAL RESEARCH

NETO2 promotes pancreatic cancer cell proliferation, invasion and migration via activation of the *STAT3* signaling pathway

This article was published in the following Dove Press journal:
Cancer Management and Research

Yaxiong Li*
Yongping Zhang*
Jiansheng Liu

Department of General Surgery, First Hospital of Shanxi Medical University, Taiyuan, 030001, Shanxi, People's Republic of China

*These authors contributed equally to this work

Purpose: The biological functions of neuropilin and tolloid-like 2 (*NETO2*) in the progression of pancreatic cancer remained unexplored. We aimed to investigate the biological roles and underlying molecular mechanisms of *NETO2* in pancreatic cancer.

Materials and methods: Thirty paired pancreatic tumor tissue samples and corresponding nontumor tissues were obtained from 30 pancreatic cancer patients who did not receive pre operative chemotherapy or radiotherapy. The changes in multiple cellular functions associated with tumor progression were assessed after *NETO2* knockdown/overexpression in pancreatic cancer cell lines. Additionally, a mouse-xenograft model was developed to verify the in vitro results.

Results: *NETO2* was upregulated in pancreatic tumor tissues. Elevated expression of *NETO2* was not only associated with an advanced tumor stage, but was also a prediction of poor prognosis for pancreatic cancer patients. Knockdown of *NETO2* in pancreatic cancer cell lines arrested the cell cycle and inhibited cell proliferation, colony formation, invasion, and migration; in contrast, overexpression of *NETO2* had an opposite effect on all of these parameters. A *STAT3* specific inhibitor, cryptotanshinone, reversed the tumor-promoting effects induced by *NETO2* overexpression in pancreatic cancer. Western blot analysis showed that invasion and migration were closely related to epithelial–mesenchymal transition, and that the *STAT3* signaling pathway was involved in *NETO2*-mediated oncogenic transformation in pancreatic cancer cells. Furthermore, *NETO2* knockdown significantly inhibited the growth of pancreatic tumor xenografts in nude mice.

Conclusion: *NETO2* has an important role in the progression and metastasis of pancreatic cancer and could serve as a novel candidate for targeted therapy of pancreatic cancer.

Keywords: pancreatic cancer, *NETO2*, proliferation, metastasis, *STAT3*

Introduction

Pancreatic cancer is a deadly malignancy with a current overall 5-year survival rate of 8%, and the major reason for its dismal survival rate has been ascribed to its early metastasis and delayed diagnosis.[1] Surgical resection, which is regarded as the only curative treatment, is not applicable for over 80% of patients in which the disease is locally advanced or metastasized.[2] For these patients, standard chemotherapy regimens—including gemcitabine-based combination chemotherapy and FOLFIRINOX chemotherapy—cannot significantly prolong survival.[3,4] A major reason for this lack of treatment efficacy is that the molecular mechanisms of pancreatic cancer carcinogenesis and metastasis remain unclear. Therefore, it is

Correspondence: Jiansheng Liu
Department of General Surgery, First Hospital of Shanxi Medical University, No. 85, Jiefangnan Road, Taiyuan, Shanxi 030001, People's Republic of China
Tel +861 840 655 7277
Email 147542533@qq.com

crucial to elucidate these molecular mechanisms and to identify early diagnostic biomarkers and potential therapeutic targets for pancreatic cancer.

Neuropilin and tolloid-like 2 (*NETO2*) gene, located on chromosome 16, encodes a single-pass transmembrane protein.[5,6] Initial studies have mainly focused on its biological functions in neural-specific processes.[7] However, subsequent reports have revealed that the expression of *NETO2* is also found in several non-neural tissues, and recent studies have further indicated that *NETO2* expression is associated with various cancers such as renal, lung, colon, cervical and colorectal cancer.[8,9] In particular, a clinical study of the relationship between dysregulation of *NETO2* expression and colorectal cancer progression has suggested that *NETO2* upregulation is associated with poor prognosis and may function as a potential biomarker of advanced carcinoma progression.[10] However, the expression pattern and biological roles of *NETO2* in pancreatic cancer remain unexplored.

The present study investigated *NETO2* expression in the tumor tissues and adjacent nontumor tissues of pancreatic cancer patients and assessed the correlation between *NETO2* expression and clinical consequences. Furthermore, we explored the biological functions of *NETO2* in proliferation, invasion, and migration of pancreatic cancer cells and their underlying molecular mechanisms.

Materials and methods

Tissue samples

This study was approved by the Ethics Committee of the First Hospital of Shanxi Medical University, and written informed consent was provided by all patients for the clinical-research use of their tumor tissues. Thirty paired pancreatic tumor tissue samples and corresponding adjacent nontumor tissues were obtained from 30 pancreatic cancer patients who did not receive preoperative chemotherapy or radiotherapy at the First Hospital of Shanxi Medical University (Taiyuan, China). The fresh tumor tissue samples and corresponding nontumor tissue samples were stored at −80 °C within 15 mins of harvesting, until further real-time quantitative PCR (qPCR) analysis.

Cell culture and reagents

Human pancreatic cancer cell lines—including PANC-1, Capan-1, AsPC-1, PATU 8988, and MIA PaCa-2—were purchased from the Shanghai Institutes for Biological Sciences (Shanghai, China). PANC-1, PATU 8988, and MIA PaCa-2 were maintained in high-glucose DMEM (Gibco, Waltham, MA, USA) supplemented with 10% FBS (Gibco) and 1% antibiotics (100 μg/mL streptomycin and 100 U/mL penicillin G); AsPC-1 was maintained in RPMI-1640 (Gibco) supplemented with 10% FBS (Gibco) and 1% antibiotics (100 μg/mL streptomycin and 100 U/mL penicillin G); Capan-1 was maintained in high-glucose DMEM (Gibco) supplemented with 15% FBS (Gibco) and 1% antibiotics (100 μg/mL streptomycin and 100 U/mL penicillin G). All cell lines were cultured at 37°C in a humidified incubator containing 5% CO_2.

Cryptotanshinone (Cat. No. S2285), a potent *STAT3* inhibitor, was purchased from Selleck, and incubated with PATU 8988 and MIA PaCa-2 at 5.8 μM for 24 hrs.

Cell transfection

Full-length *NETO2* cDNA (GenBank accession number NM_001201477.1) was subcloned into an expression vector (pcDNA3.1/+) using the primer sequences 5'-AGCTGCTCCACGTCAAAGAA-3' and 5'-GCTCCC-GAGAGCTCGAA-3'. Then, a *NETO2* overexpression plasmid and control vector (ie an empty pcDNA3.1/+ plasmid) was transfected into MIA PaCa-2 and PATU 8988 cells. The *NETO2* expression level was examined by western blot.

The sequences of the siRNA specifically targeting *NETO2* and its negative control (NC) were 5′-GCAGGAGUAUUUGAACAAA-3′ and 5′-TTCTC-CGAACGTGTCACGT-3′, respectively. A lentivirus-*NETO2*-shRNA (lv-sh*NETO2*) that expressed *NETO2*-siRNA and a lentivirus-NC-shRNA (lv-shNC) that expressed NC-siRNA were purchased from Genechem (Shanghai, China). These lentiviruses—which contained puromycin resistance and a green-fluorescent protein reporter gene—were then stably transfected into PANC-1 and Capan-1 cells over 48 hrs at a multiplicity of infection of 50. These transfected cells were selected by puromycin (2 μg/mL) for 3 days and were used in subsequent experiments.

Quantitative real-time PCR

Total RNA was extracted from tissue samples and cultured cells using TRIzol reagent (Invitrogen, Waltham, MA, USA). Then, a reverse transcription reagent kit (TaKaRa, Dalian, China) was used to synthesize the cDNA. Quantitative real-time PCR was performed to amplify the target genes and measure their expression with glyceraldehyde 3-phosphate dehydrogenase (*GAPDH*) as an internal loading control. The SYBR-Green method was used according to the manufacturer's instructions for this

process and the results were analyzed with the $2^{-\Delta\Delta CT}$ method described previously.[11]

Western blot analysis

Cells were lysed in RIPA buffer (Beyotime, Shanghai, China) with a phosphatase inhibitor cocktail and protease inhibitor. After measuring the concentration of the extracted proteins with a BCA Protein Assay kit (Beyotime), equal amounts of protein were separated by SDS-PAGE and then transferred to polyvinylidene difluoride membranes. Membranes were then blocked with 5% skim milk. After 1 hr of blocking, the membranes were incubated at 4°C overnight with the following primary antibodies: anti-NETO2 (1:200; Abcam), anti-N-cadherin (1:1,000; CST), anti-E-cadherin (1:1,000; CST), anti-vimentin (1:1,000; CST), STAT3 (1:1,000; CST), phospho-STAT3 (p-STAT3) (Tyr705) (1:1,000; CST), Cyclin D1 (1:1,000; CST) and the internal control anti-GAPDH (1:5,000; Abways). After being washed in TBST three times, the membranes were incubated for 1 hr at room temperature with a secondary antibody (goat anti-mouse/anti-rabbit IgG-HRP; 1:2,000, Abcam). The bands were visualized with a chemiluminescent substrate enhanced chemiluminescence kit according to the manufacturer's instruction.

Cell proliferation assay

Cell proliferation was quantitatively analyzed by cell counting kit-8 (CCK8) assay (Dojindo, Japan) according to the manufacturer's instructions. The OD was detected at the wavelength of 450 nm using a microplate reader (TEK,Bio-Saxony, USA).

Colony formation assay

The same number of transfected and non-transfected cells were separately seeded at a density of 500 cells/well into 6-well plates. The cells were subsequently cultured on the plates for 2–3 weeks. Then, the cell colonies (>50 cells/colony) were counted and photographed after crystal violet staining.

Cell cycle analysis

Cells were seeded and cultured in 6-well plates. Forty-eight hours after transfection, the cells were collected and then fixed with chilled 70% ethanol at 4°C for 12 hrs. Subsequently, the cells were stained with propidium iodide (Sigma-Aldrich, St Louis, MO, USA) at room temperature in the dark for 30 min and then analyzed by flow cytometry (BD Biosciences, San Jose, CA, USA).

Cell invasion and migration assays

Cell invasion and migration capability were evaluated using transwell chambers (pore size of 8 μm; Corning Incorporated, Corning, NY, USA) with Matrigel and without Matrigel, respectively. The same number of differently treated cells were separately resuspended in 200 μL of serum-free DMEM and then plated in the upper chambers (PANC-1, 2×10^4; Capan-1, 5×10^4; PATU 8988, 3×10^4; and MIA PaCa-2, 3.5×10^4). The lower chambers were loaded with 600 μL of DMEM/10% FBS media. After incubation for 24 hrs (migration assay) or 48 hrs (invasion assay), the cells were fixed with 4% paraformaldehyde and then stained with 0.1% crystal violet. Five random visual fields at 100× magnification were selected for quantification of penetrated cells in each well.

Mouse xenograft model

A suspension of PANC-1 (5×10^6) cells transfected with lv-sh*NETO2* or lv-shNC were injected into the right flank of 4- to 6-week-old male BALB/c nude mice (Slac, Shanghai, China) which were cared for under standard conditions in accordance with the guidelines of First Hospital of Shanxi Medical University Ethics Committee. Tumor volume was calculated every week by measuring the tumor width and length and then employing the equation: $V=4\pi/3\times (\text{width}/2)^2 \times (\text{length}/2)$. After 30 days, the mice were sacrificed and the tumors were collected and weighed. In this study, all animal experiments were approved by the First Hospital of Shanxi Medical University Ethics Committee.

Immunohistochemical staining

After collection and weighing, the xenograft tumors were immediately fixed in 10% formalin. Subsequently, the tumors were embedded in paraffin and cut into 5-mm sections with the following steps. Briefly, these sections were incubated with the anti-Ki67 primary antibody (1:400; Abcam) at 4°C overnight and a goat anti-rabbit-peroxidase-conjugated secondary antibody (1:1,000; Santa Cruz Biotechnology Inc., Dallas, TX, USA) at room temperature for 1 hr, successively. Then, a DAB Substrate Kit (Maxin) was used for the following immunohistochemical staining according to the manufacturer's instructions and staining results were observed and imaged through a light microscope.

Statistical analysis

All experiments were conducted three times and statistical analyses were performed using GraphPad Prism 5 (GraphPad Software, Inc., La Jolla, CA, USA) and SPSS

19.0 software (SPSS Inc., Chicago, IL, USA). Quantified values are expressed as the mean ± SD. χ^2 tests and independent Student's *t*-tests were used to evaluate the effects of *NETO2* on pancreatic cancer cell lines. Survival analysis was performed with Kaplan-Meier analysis. $P<0.05$ (*$P<0.05$, **$P<0.01$, ***$P<0.001$) was considered to represent statistical significance.

Results

NETO2 is upregulated in pancreatic tumor tissues and correlates with poor survival

To determine the expression pattern of *NETO2* in pancreatic tumor tissues, we conducted real-time qPCR analysis to compare the relative mRNA levels of *NETO2* in 30 pairs of matched pancreatic tumor tissue samples. *NETO2* was significantly upregulated in pancreatic tumor tissues compared with that of adjacent nontumor tissues (Figure 1A and B). Furthermore, these pancreatic tumor tissue samples were divided into three groups (stage I, stage II and stage III-IV) according to the current American Joint Committee on Cancer (AJCC) staging system. The results of real-time qPCR analysis showed that mRNA levels of *NETO2* in later-stage groups were significantly higher than those in lower stage groups (Figure 1C). This correlation suggested that *NETO2* may be closely linked with pancreatic cancer progression and development. In addition, we divided these pancreatic tumor samples into two groups according to the expression of *NETO2* (ie, high/low *NETO2* expression groups) by setting the median *NETO2* expression level as the cutoff point. Kaplan-Meier analysis showed that higher *NETO2* expression was correlated with worse overall survival (Figure 1D).

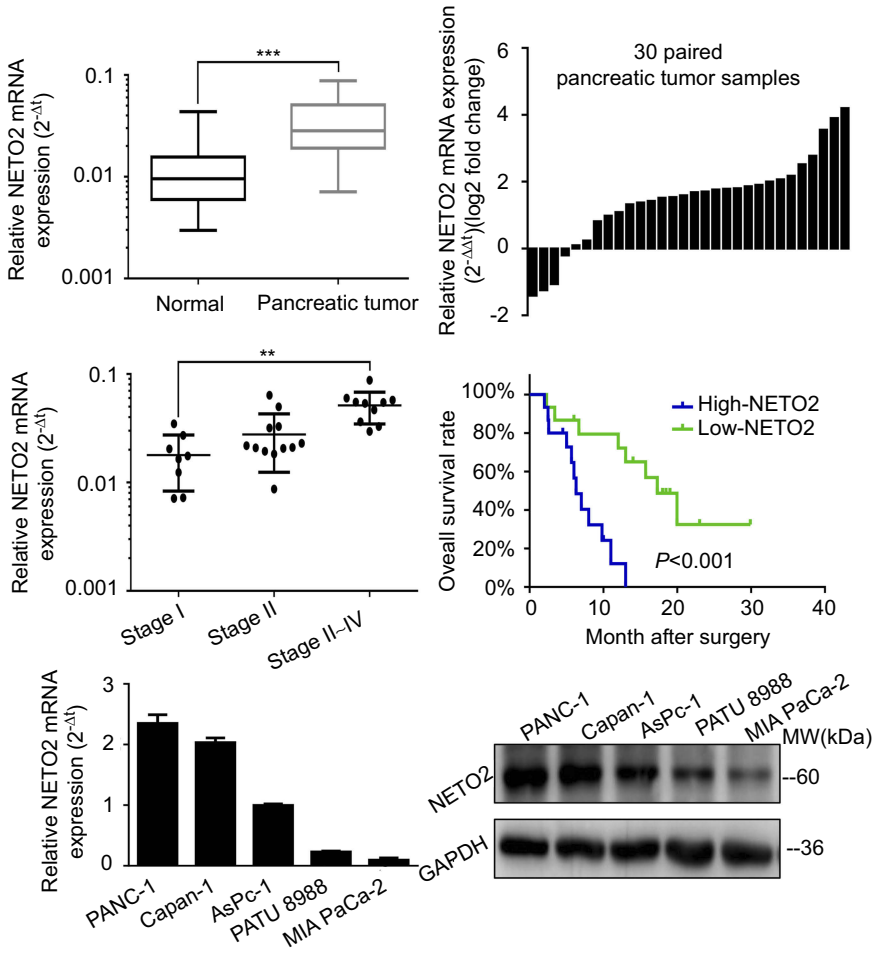

Figure 1 *NETO2* expression and its significance in pancreatic tumor tissues and cell lines.

Notes: (**A**) Relative *NETO2* mRNA levels in 30 pancreatic tumor tissue samples and adjacent nontumor tissues. ***$P<0.001$. (**B**) Comparison of *NETO2* mRNA levels between pancreatic tumor tissues and their corresponding adjacent nontumor tissues. (**C**) Relative *NETO2* mRNA levels in three different cancer stages of pancreatic tumor samples. **$P<0.01$. (**D**) Kaplan-Meier overall survival curve of pancreatic cancer patients with high ($n=15$) and low ($n=15$) *NETO2* mRNA levels. ***$P<0.001$. (**E**) Relative *NETO2* mRNA levels in five pancreatic cancer cell lines. (**F**) Relative NETO2 protein levels in five pancreatic cancer cell lines.

These clinical data suggest that *NETO2* is upregulated in pancreatic cancer and that this upregulation is associated with an advanced tumor stage and poor prognosis.

Different *NETO2* expression levels in various pancreatic cancer cell lines

To explore the biological function of *NETO2* in pancreatic cancer cells, we first conducted real-time qPCR and western blot assays to assess *NETO2* expression levels in five pancreatic cell lines (Figure 1E and F). The results showed that *NETO2* was differentially expressed both at mRNA and protein levels. Specifically, PANC-1 and Capan-1 cells expressed higher levels of *NETO2* compared with those in MIA PaCa-2 and PATU 8988 cells. Thus, for further functional experimentation, we selected PANC-1 and Capan-1 cell lines to construct knockdown models and MIA PaCa-2 and PATU 8988 cell lines to construct overexpression models. *NETO2* expression was determined by using western blot analysis (Figure 2A and B).

NETO2 enhances proliferative capability of pancreatic cancer cells in vitro

CCK8 and colony formation assays were performed to assess the effects of *NETO2* in pancreatic cancer cells. As CCK8 assays showed, *NETO2* knockdown restrained the proliferation of PANC-1 and Capan-1 cells (Figure 2C). Similarly, we obtained the same results from colony assays in that the number of colonies was significantly reduced after *NETO2* knockdown (Figure 2E and G). In contrast, *NETO2* overexpression in MIA PaCa-2 and PATU 8988 cells displayed the opposite pattern in that cell proliferation and the number of colonies were significantly increased (Figure 2D, F and G). These results demonstrate that *NETO2* expression enhances the proliferative capability of pancreatic cancer cells.

NETO2 knockdown suppresses pancreatic tumor growth in vivo

We then explored the effects of *NETO2* on tumor growth. Compared with the NC group, tumor volume and weight were significantly reduced in the *NETO2*-knockdown group (Figure 2H and I). Immunohistochemical staining also showed that the expression of the cell proliferation marker, *Ki-67*, in the *NETO2*-knockdown group was lower than in the NC group (Figure 2J and K). These results suggested that *NETO2* may play an important role in pancreatic tumor growth in vivo.

NETO2 promotes pancreatic cancer cell invasion and migration by regulation of the epithelial–mesenchymal transition

In order to explore the role of *NETO2* in changes to pancreatic tumor aggressiveness, we performed invasion and migration transwell assays. Since the expression level of *NETO2* also influenced cell proliferation, we first conducted statistical analysis of the 24/48 hr CCK8 data to evaluate the effect of cell proliferation on the results. The result showed that there were no statistical differences in the cell proliferation level between different treatment groups after cells were cultured for 24 h/48 h, which meant that the differences of penetrated cell number between different treatment groups were due to cell migration (24 hr)/invasion (48 hr) rather than cell proliferation. As shown in Figure 3A, *NETO2* knockdown remarkably impaired the invasive and migratory capacities of PANC-1 and Capan-1 cells. Corresponding to the above results, *NETO2* overexpression increased the invasiveness and migratory capacities of MIA PaCa-2 and PATU 8988 cells (Figure 3B). Given that tumor cell invasion and migration is usually associated with epithelial–mesenchymal transition (EMT), we assessed the expression of EMT-associated markers by western blot analysis. As shown in Figure 3C, *NETO2* knockdown in PANC-1 and Capan-1 cells increased *E-cadherin* expression, but reduced the expression of *N-cadherin* and *vimentin*. Remarkably, *NETO2* overexpression in MIA PaCa-2 and PATU 8988 cells caused the opposite results. Such findings suggest that *NETO2* promotes pancreatic cancer cell invasion and migration by regulation of EMT.

NETO2 accelerates cell cycle progression of pancreatic cancer

We investigated the effects of *NETO2* on cell cycle progression to further explore the promoting function of *NETO2* on cell proliferation. *NETO2* knockdown, both in PANC-1 and Capan-1 cells, led to more cells remaining in G1 phase because the cell cycle transition from G1 to S phase was blocked, thus inhibiting cell proliferation (Figure 3D). In contrast, *NETO2* overexpression in MIA PaCa-2 and PATU 8988 cells induced the converse effect (Figure 3E).

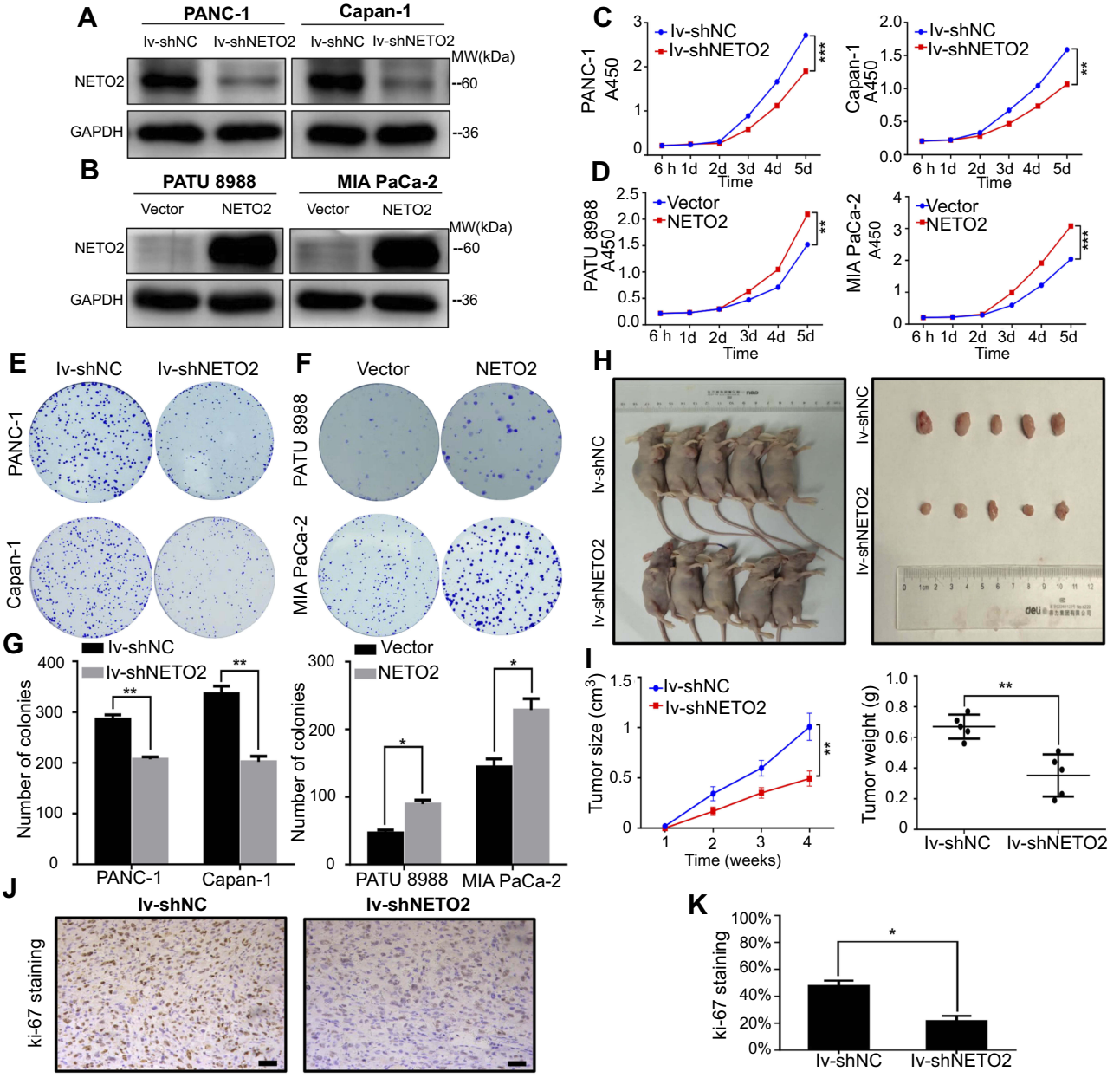

Figure 2 Effect of *NETO2* knockdown and overexpression on the proliferation of pancreatic cancer cells.

Notes: (**A** and **B**) Relative *NETO2* protein levels in PANC-1 and Capan-1 cells infected with lv-sh*NETO2*/lv-shNC. (**A**) Relative *NETO2* protein levels in PATU 8988 and MIA PaCa-2 cells transfected with control or *NETO2*-expressing plasmid (**B**). GAPDH served as the internal control. (**C** and **D**) Cell proliferation was assessed after *NETO2* knockdown (**C**) and overexpression (**D**) in pancreatic cancer cell lines with CCK8 assays. ***P*<0.01, ****P*<0.001. (**E** and **F**) Colony-formation capability was assessed in pancreatic cancer cell lines with *NETO2* knockdown (**E**) or overexpression (**F**). (**G**) The number of colonies was counted; scale bar = 100 μm. **P*<0.05, ***P*<0.01. (**H**) Representative results after a mouse were injected with differentially treated PANC-1 cells (infected with lv-sh*NETO2*/lv-shNC) and the corresponding tumors. (**I**) Tumor size and weight were analyzed quantitatively. ***P*<0.01. (**J** and **K**) IHC analysis of Ki-67 expression in xenograft tumors; scale bar = 100 μm. **P*<0.05.

Abbreviations: lv, lentivirus; NC, negative control; IHC, immunohistochemistry; CCK8, cell counting kit-8.

Furthermore, we examined the expression level of Cyclin D1, a key cell cycle regulating protein. As shown in Figure 3F, we found that Cyclin D1 expression levels in *NETO2*-knockdown cells were lower than that in NC cells. Additionally, *NETO2*-overexpressed cells had higher expression levels of Cyclin D1 protein than that in NC cells. Taken together, these results demonstrate that *NETO2* accelerates the cell cycle progression of pancreatic cancer.

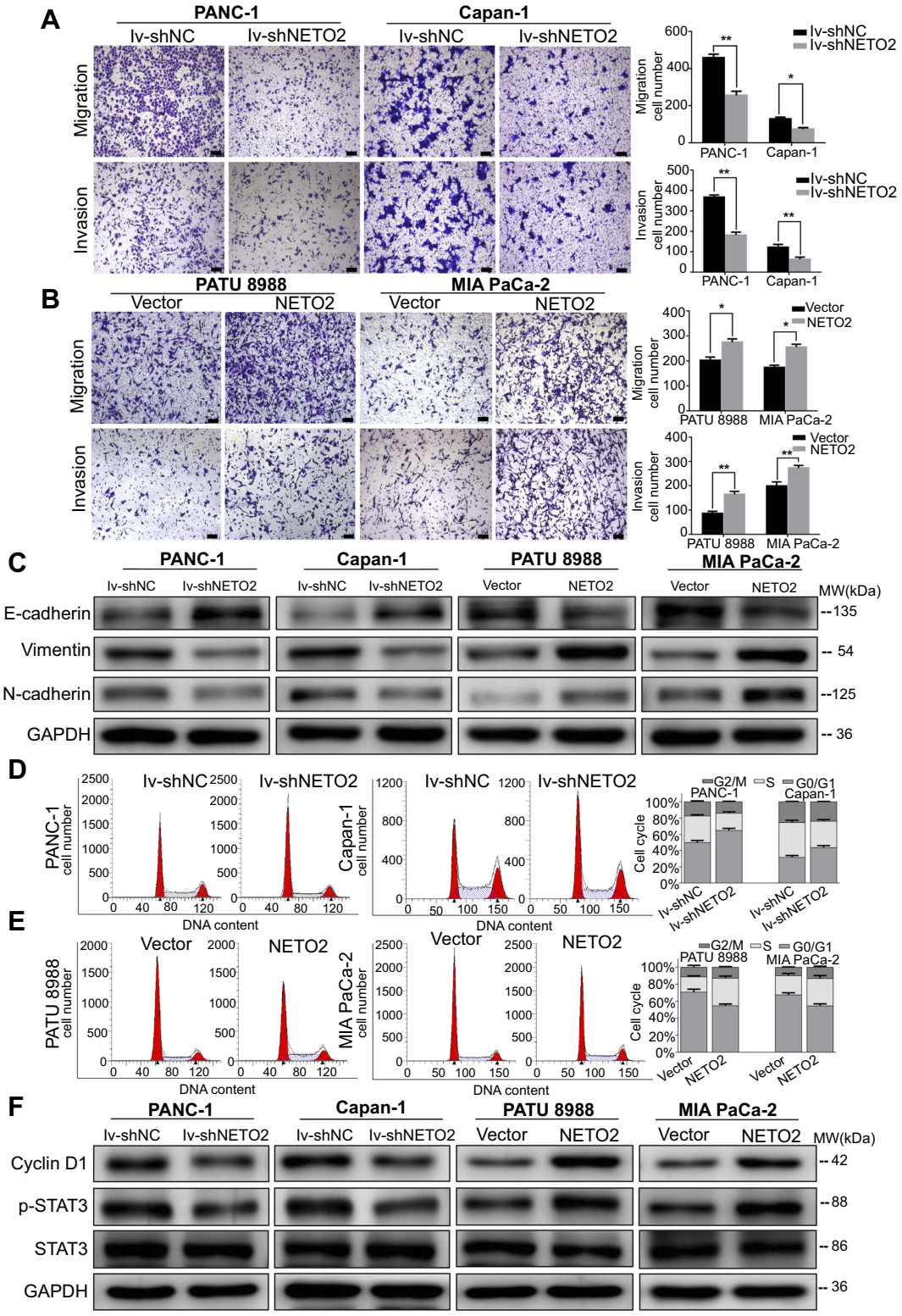

Figure 3 Effects of *NETO2* knockdown and overexpression on migration, invasion and cell cycle progression of pancreatic cancer cells.

Notes: (**A** and **B**) Migration and invasion analysis of pancreatic cancer cell lines with *NETO2* knockdown (**A**) or overexpression (**B**). Scale bar =100 μm. **P*<0.05, ***P*<0.01. (**C**) Western blot analysis of E-cadherin, vimentin and N-cadherin. GAPDH was used as a loading control. (**D** and **E**) Cell cycle analysis of pancreatic cancer cell lines with the *NETO2* knockdown (**D**) or overexpression (**E**). The *x*-axis represents the cell cycle distribution, and the *y*-axis represents the cell number. (**F**) Western blot analysis of Cyclin D1, p-STAT3, STAT3. GAPDH was used as a loading control.

Abbreviations: lv, lentivirus; NC, negative control.

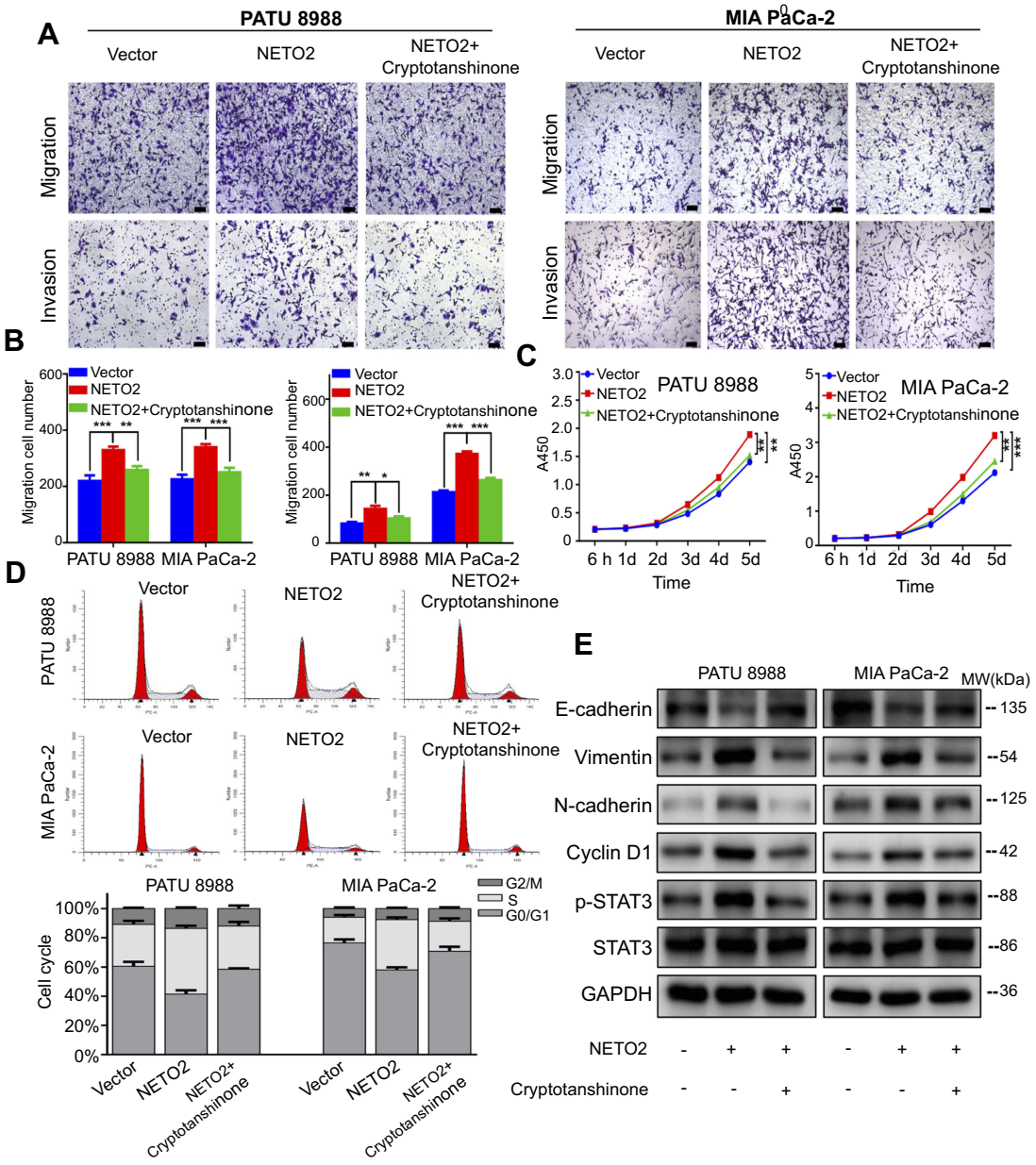

Figure 4 Suppression of STAT3 phosphorylation antagonizes *NETO2*-mediated pancreatic cancer cell proliferation, invasion and migration.

Notes: (**A** and **B**) Invasion and migration assays for *NETO2*-overexpressed pancreatic cancer cells with or without 5.8 μM cryptotanshinone treatment. Scale bar = 100 μm. **P*<0.05, ***P*<0.01, ****P*<0.001. (**C**) CCK8 assay for *NETO2*-overexpressed pancreatic cancer cells with or without 5.8 μM cryptotanshinone treatment. ***P*<0.01, ****P*<0.001. (**D**) Cell cycle analysis of *NETO2*-overexpressed pancreatic cancer cells with or without 5.8 μM cryptotanshinone treatment. The *x*-axis represents the cell cycle distribution, and the y-axis represents the cell number. (**E**) Western blot analysis of E-cadherin, vimentin, N-cadherin, Cyclin D1, p-STAT3, and STAT3 for *NETO2*-overexpressed pancreatic cancer cells with or without 5.8 μM crytotanshinone treatment. GAPDH was used as a loading control.

Abbreviations: lv, lentivirus; NC, negative control; CCK8, cell counting kit-8.

NETO2 regulates the *STAT3* signaling pathway in pancreatic cancer cells

To further elucidate the underlying mechanism of *NETO2* in pancreatic cancer cells, we compared the expressions of several cell proliferation-associated genes upstream of *Cyclin D1* by western blot analysis. We found that *NETO2* knockdown decreased the phosphorylation of STAT3, while *NETO2* overexpression increased STAT3 activation (Figure 3F). Thus, we speculated that *NETO2* might be associated with the *STAT3* signaling pathway in pancreatic cancer cells. The *STAT3* inhibitor cryptotanshinone was used for further exploration. As shown in Figure 4A and B, cryptotanshinone blocked *NETO2*-mediated cell invasion and migration in these cancer cells. Likewise, CCK8 assays and cell cycle analysis revealed that

cryptotanshinone treatment inhibited *NETO2*-mediated cell proliferation in MIA PaCa-2 and PATU 8988 cells (Figure 4C and D). Consistently, western blot analysis showed that cryptotanshinone reversed the effects of *NETO2* overexpression on the expression of *Cyclin D1*, *E-cadherin*, *vimentin*, *N-cadherin*, and *p-STAT3* (Figure 4E). These results suggest that *NETO2* enhances the capabilities of proliferation, invasion and migration of pancreatic cancer cells by activation of the *STAT3* pathway.

Discussion

Previous studies of *NETO2* have mainly focused on its neurobiological aspects. Nevertheless, the association between elevated expression of *NETO2* and malignant tumor transformation has been subsequently revealed for many types of tumors. In the present study, we found that *NETO2* was upregulated in pancreatic cancer tissues compared with adjacent nontumor tissues. Moreover, the elevated expression of *NETO2* was associated with an advanced tumor stage of pancreatic cancer patients and indicated poor prognosis. These results are in line with previous studies that have indicated that increased *NETO2* expression can be detected in various cancers and may contribute to early diagnosis.[8–10] Therefore, *NETO2* could serve as a potential therapeutic target in pancreatic cancer and may be useful for diagnosis and prognosis.

STAT3, a member of the *STAT* family, has been identified as a critical transcription factor in the malignant transformation of many types of tumors.[12–14] Upstream stimuli activate the *STAT3* signaling pathway through promotion of STAT3 phosphorylation. The increased phosphorylation at Tyr 705 of STAT3 induces the interaction of the SH2 domain and phosphotyrosine, thereby causing STAT3 dimerization and the following translocation to the nucleus. Once within the nucleus, dimerized STAT3 regulates the expression of target genes related to proliferation and metastasis, such as *Cyclin D1*.[15,16] In the present study, we demonstrated that *NETO2* knockdown induced G0/G1 phase cell cycle arrest and thus inhibited pancreatic cancer cell proliferation by reducing the phosphorylation of STAT3 and subsequently attenuating the expression of *Cyclin D1*.

The EMT process has been demonstrated to be required for invasion and metastasis in many types of human cancers.[17–19] In the EMT process, which is also considered to be regulated by many signaling pathways, including the *STAT3* signaling pathway,[20] epithelial cells lose their epithelial properties, such as decreased expression of epithelial markers (eg, *E-cadherin*), and gain mesenchymal phenotypes, such as increased expression of mesenchymal markers (eg, *vimentin*, *N-cadherin*).[21,22] In the present study, we found that *NETO2* participates in the regulation of EMT through the *STAT3* signaling pathway which alters the expression of these EMT-related proteins. It should be noted that a previous study indicated there was no significant correlation between the mRNA expression levels of *NETO2* gene and EMT-related genes in colorectal cancer tissues.[8] The possible reasons for this discrepancy include the following: (1) the effects of *NETO2* on EMT vary between cancer types; (2) non-tumor cells in tumor tissues may interfere with real-time qPCR analysis of EMT-related genes at the mRNA level; and (3) a different selection of samples may have a different impact on the results. To summarize, we argue that *NETO2* upregulation drives the process of EMT by activating the STAT3 signaling pathway and hence promotes invasion and migration of pancreatic cancer cells. Our research further demonstrated that *NETO2*-mediated oncogenic function in pancreatic cancer cells could be reversed by cryptotanshinone (a *STAT3*-specific inhibitor) via inhibition of STAT3 phosphorylation. Furthermore, we found that *NETO2* knockdown could significantly inhibit tumor growth in vivo in nude mice.

Conclusion

NETO2 acts as an oncogenic gene in pancreatic cancer by activating the *STAT3* signaling pathway. The detection of *NETO2* expression may provide help for early diagnosis and prognosis of pancreatic cancer. We also argue that *NETO2* could serve as a novel candidate for targeted therapy of pancreatic cancer.

Acknowledgments

We are grateful to Prof. Liu Yingbin and his research group for their generous help in providing experimental guidance. We also thank Dr. Hu Yunping and Dr. Song Xiaoling for editing the revised manuscript.

Disclosure

The authors report no conflicts of interest in this work.

References

1. Siegel RL, Miller KD, Jemal A. Cancer statistics, 2018. *CA Cancer J Clin*. 2018;68(1):7–30. doi:10.3322/caac.21442

2. Teague A, Lim KH, Wang-Gillam A. Advanced pancreatic adenocarcinoma: a review of current treatment strategies and developing therapies. *Ther Adv Med Oncol*. 2015;7(2):68–84. doi:10.1177/1758834014564775
3. Cid-Arregui A, Juarez V. Perspectives in the treatment of pancreatic adenocarcinoma. *World J Gastroenterol*. 2015;21(31):9297–9316. doi:10.3748/wjg.v21.i31.9297
4. Mian OY, Ram AN, Tuli R, et al. Management options in locally advanced pancreatic cancer. *Curr Oncol Rep*. 2014;16(6):388–482. doi:10.1007/s11912-014-0388-y
5. Finelli P, Sirchia SM, Masciadri M, et al. Juxtaposition of heterochromatic and euchromatic regions by chromosomal translocation mediates a heterochromatic long-range position effect associated with a severe neurological phenotype. *Mol Cytogenet*. 2012;5(1):16. doi:10.1186/1755-8166-5-16
6. Stohr H. A novel gene encoding a putative transmembrane protein with two extracellular CUB domains and a low-density lipoprotein class A module: isolation of alternatively spliced isoforms in retina and brain. *Gene*. 2002;286(2):223–231. doi:10.1016/S0378-1119(02)00438-9
7. Ivakine EA, Acton BA, Mahadevan V, et al. Neto2 is a KCC2 interacting protein required for neuronal Cl- regulation in hippocampal neurons. *Proc National Acad Sci*. 2013;110(9):3561–3566. doi:10.1073/pnas.1212907110
8. Fedorova MS, Snezhkina AV, Pudova EA, et al. Upregulation of NETO2 gene in colorectal cancer. *BMC Genet*. 2017;18(S1):117. doi:10.1186/s12863-017-0581-8
9. Niu O, Sadritdinova AF, Snezhkina AV, et al. [Increase in NETO2 gene expression is a potential molecular genetic marker in renal and lung cancers]. *Genetika*. 2012;48(5):506–512. doi:10.1134/S1022795412050171
10. Hu L, Chen HY, Cai J, et al. Upregulation of NETO2 expression correlates with tumor progression and poor prognosis in colorectal carcinoma. *BMC Cancer*. 2015;15(1):1006. doi:10.1186/s12885-015-2018-y
11. Xiaoling S, Minghui Z, Fahong Z, et al. ZFX promotes proliferation and metastasis of pancreatic cancer cells via the MAPK pathway. *Cell Physiol Biochem*. 2018;48(1):274–284. doi:10.1159/000491727
12. Banerjee K, Resat H. Constitutive activation of STAT3 in breast cancer cells: a review. *Int J Cancer*. 2016;138(11):2570–2578. doi:10.1002/ijc.29923
13. Fukuda A, Wang S, Morris JP 4th, et al. Stat3 and MMP7 contribute to pancreatic ductal adenocarcinoma initiation and progression. *Cancer Cell*. 2011;19(4):441–455. doi:10.1016/j.ccr.2011.03.002
14. Surana R. Targeting the STAT3 signaling pathway in cancer: role of synthetic and natural inhibitors. *Biochim Biophys Acta*. 2014;1845(2):136–154. doi:10.1016/j.bbcan.2013.12.005
15. Yu H, Jove R. The STATs of cancer–new molecular targets come of age. *Nat Rev Cancer*. 2004;4:97–105. doi:10.1038/nrc1275
16. Zhang Z, Duan Q, Zhao H, et al. Gemcitabine treatment promotes pancreatic cancer stemness through the Nox/ROS/NF-κB/STAT3 signaling cascade. *Cancer Lett*. 2016;382(1):53–63. doi:10.1016/j.canlet.2016.08.023
17. Hu YP, Wu ZB, Jiang L, et al. STYK1 promotes cancer cell proliferation and malignant transformation by activating PI3K-AKT pathway in gallbladder carcinoma. *Int J Biochem Cell Biol*. 2018;97:16–27. doi:10.1016/j.biocel.2018.01.016
18. Jin, YJ, Li F, Zheng C, et al. NEDD9 promotes lung cancer metastasis through epithelial- mesenchymal transition. *Int J Cancer*. 2014;134(10):2294–2304. doi:10.1002/ijc.28568
19. Bethany S, Neil B. Role of EMT in metastasis and therapy resistance. *J Clin Med*. 2016;5(2):17. doi:10.3390/jcm5020017
20. Liu RY, Liu RY, Zeng Y, et al. JAK/STAT3 signaling is required for TGF-β-induced epithelial-mesenchymal transition in lung cancer cells. *Int J Oncol*. 2014;44(5):1643–1651. doi:10.3892/ijo.2014.2310
21. Pavelic SK, Sedic M, Bosnjak H, et al. Metastasis: new perspectives on an old problem. *Mol Cancer*. 2011;10:22. doi:10.1186/1476-4598-10-22
22. Lee JM, Dedhar S, Thompson KEW. The epithelial-mesenchymal transition: new insights in signaling, development, and disease. *J Cell Biol*. 2006;172(7):973–981. doi:10.1083/jcb.200601018